

Photophysical and Photochemical Properties of New Coumarin-Substituted Zinc and Indium Phthalocyanines for Photodynamic Therapy

Zehra Kazancıçok¹ , Mustafa Bulut² , Ümit Salan^{3*} 

^{1,2,3}Marmara University, Department of Chemistry, 34722 Istanbul, Türkiye.

* usalan@marmara.edu.tr

* Orcid No: 0000-0003-0379-1066

Received: November 8, 2024

Accepted: January 30, 2025

DOI: 10.18466/cbayarfbe.1581909

Abstract

In this study, we synthesized and characterized zinc (II) and indium (III) acetate phthalocyanine derivatives, modified with 7-hydroxy-8-methyl-4-(2,3,4,5-tetrafluorophenyl)coumarin, as potential photosensitizers for photodynamic therapy (PDT). The synthesized phthalocyanines were characterized using various analytical techniques, including elemental analysis, UV-Vis, FT-IR spectroscopy, and MALDI-TOF mass spectrometry. The study focused on the photophysical and photochemical properties of these compounds, particularly their singlet oxygen and photodegradation quantum yields. Zinc phthalocyanine exhibited lower fluorescence quantum yield and higher stability, whereas indium phthalocyanine showed superior singlet oxygen generation. These findings suggest that coumarin-substituted phthalocyanines hold promise as effective photosensitizers in PDT, with indium derivatives demonstrating enhanced photodynamic efficacy.

Keywords: Coumarin, Phthalocyanine, Photodynamic therapy, PDT, Singlet oxygen.

1. Introduction

Phthalocyanines (Pcs) are macrocyclic compounds with a planar structure formed by the condensation of four iminoisoindoline units, featuring an 18 π -electron delocalization system and there is good structural flexibility in both free-metal (H_2Pcs) and metal complexes of Pcs (MPcs). Up to 70 different elements can reside in the central cavity of Pcs, which in certain circumstances can allow for the functionalization of metal-axial ligands to modify the structure. Moreover, different substituents can be incorporated into the core of Pcs at the non-peripheral (α) and peripheral (β) places to yield a range of electrical characteristics [1]. Due to their extensive range of applications, they are used in various fields, including optical data storage devices [2], semiconductors [3], [4], solar cells [5], [6], gas sensors [7], and liquid crystals [8], [9]. Their versatility is largely attributed to the 18 π -electron delocalization system [10]. In addition, phthalocyanines are employed in cancer photodynamic therapy (PDT) as second-generation photosensitizers [11]. The primary benefits of these compounds include their high absorption capacity within the visible spectrum, efficient singlet oxygen generation, and their susceptibility to chemical modifications. These properties highlight the significant potential of

phthalocyanines in diverse technological and medical applications [12], [13].

The efficacy of phthalocyanines in photodynamic therapy can be significantly enhanced by incorporating diamagnetic metal ions. Metals like Mg^{2+} , Zn^{2+} , Al^{3+} , Ga^{3+} , In^{3+} , Si^{4+} , and Lu^{3+} within the phthalocyanine core are particularly effective, as they promote the production of singlet oxygen, thus boosting the therapeutic efficiency [14], [15], [16], [17]. Additionally, modifying the photophysical and photochemical properties of phthalocyanines can be achieved by strategically introducing functional groups at various positions within their cyclic Structure [18].

In recent years, photodynamic therapy (PDT) has emerged as a significant method for cancer treatment, relying on three key components: a photosensitizer, light, and oxygen. The mechanism of PDT involves the interaction between the light-activated photosensitizer and nearby molecules [19]. This interaction generates singlet oxygen (1O_2), which can damage biological substrates and ultimately cause cell death. Compounds with macrocyclic structures, such as phthalocyanines, are highly effective in indirectly producing singlet oxygen due to their ability to persist in a triplet excited state [20].

The diversification of central metals allows for the synthesis of numerous new compounds. In this context, phthalocyanines emerge as promising compounds in cancer photodynamic therapy [21].

Coumarin and its derivatives have recently attracted attention as oxygenated heterocyclic compounds with an aromatic-heterocyclic structure containing a lactone ring [22]. These compounds, found in nature as secondary plant metabolites [23], are utilized in various medical and biological applications as antiviral [24], antibacterial [25], anticoagulant [26], antioxidant [27], anti-enzymatic [28], and anticancer agents [29], [30]. When combined with phthalocyanines, known as effective photosensitizers, they form complex structures that may exhibit similar properties [31]. Coumarin derivatives, especially those with a hydroxyl group at the 7-position and substitutions at the 4-position, are also intriguing due to their photochemical and photophysical properties [32]. These properties render them useful in various applications such as whitening agents [33], optical chromophores [34], laser dyes [35], and solar energy collectors [36]. Considering the biological significance of coumarin and phthalocyanine derivatives, the synthesis of compounds by combining these functional molecules via synthetic methods and evaluating their ability to produce singlet oxygen has recently garnered significant interest [37], [38], [39].

In this study, indium (III) acetate and zinc (II) phthalocyanine derivatives, modified with 7-hydroxy-8-methyl-4-(2,3,4,5-tetrafluorophenyl)coumarin compounds, were used as photosensitive dyes for photodynamic therapy in cancer treatment. Phthalocyanine compounds were synthesized and characterized using a range of analytical techniques, including elemental analysis, UV-Vis spectroscopy, FT-IR, ¹H-NMR, ¹³C-NMR, ¹⁹F-NMR, and MALDI-TOF mass spectrometry. This study centered on characterizing and examining the photophysical and photochemical properties of these compounds. Furthermore, comparisons with previous studies were conducted to assess how different substituent binding positions on the phthalocyanine skeleton and the role of central metal ions within the phthalocyanine cavity influence the properties of the compounds.

2. Materials and Methods

2.1. Materials

All chemicals used for the syntheses are of reagent grade quality. 3-Nitrophthalonitrile, 7-hydroxy-8-methyl-4-(2,3,4,5-tetrafluorophenyl)coumarin (**1**), and 7-(2,3-dicyanophenoxy)-8-methyl-4-(2,3,4,5-tetrafluorophenyl)coumarin (**2**) were synthesized and purified according to the methods previously described in the literature [40], [41]. 2-Methylresorcinol, ethyl-(2,3,4,5-tetrafluorobenzoyl)acetate, potassium

carbonate, 1,3-diphenylisobenzofuran (DPBF), and metal salts were purchased from Sigma-Aldrich and used as received. All reactions were conducted under a high-purity nitrogen atmosphere. The ZnPc (**3**) and InPc (**4**) compounds were purified through Soxhlet extraction with hot acetic acid, water, ethanol, and acetonitrile. For further purification, column chromatography on silica gel 60 (0.040-0.063 mm) was employed. The melting points of the phthalocyanine compounds were observed to be above 300 °C. The purity of the substances was checked at each stage using thin-layer chromatography (TLC, Silica gel 60 F254).

2.2. Equipments

FT-IR spectra were recorded using a Perkin Elmer Spectrum 100 FT-IR Spectrometer. Deuterated DMSO-d₆ for NMR studies was sourced from Merck. ¹H, ¹³C, and ¹⁹F-NMR spectra were measured with a Bruker DPX 400 MHz spectrometer. Mass spectra were acquired using a Bruker Microflex LT MALDI-TOF Mass Spectrometer equipped with a nitrogen UV laser operating at 337 nm, with dithranol (DIT) and 2,5-dihydroxybenzoic acid (DHB) used as matrices. The LECO CHNS-932 elemental analyzer was used to carry out the microanalyses of C, H, and N. A Shimadzu UV-2450 UV-Visible Spectrophotometer was used to record optical spectra in the UV-visible range. Fluorescence lifetimes were determined using a time-correlated single-photon counting (TCSPC) setup with Horiba Fluorolog 3 equipment. Emission and excitation spectra of fluorescence were recorded using a Hitachi F-7000 spectrofluorometer with a 1 cm path length cuvette. To perform photo-irradiations, a 300W-120V Osram optic halogen lamp was used. UV and infrared radiations were filtered using a water filter and a Schott glass cut-off filter (600 nm), respectively. In addition, an interference filter (Intor) with a 670–700 nm bandwidth was positioned in front of the sample. A POWER MAX PM5100 laser power meter was used to measure the intensities of the light (Moletron detector included).

2.3. Synthesis

4-Nitrophthalonitrile was synthesized and purified using methods described in the literature [40], [41]. 7-Hydroxy-8-methyl-4-(2,3,4,5-tetrafluorophenyl)coumarin (**1**) was prepared via the Pechmann reaction. 7-(2,3-Dicyanophenoxy)-8-methyl-4-(2,3,4,5-tetrafluorophenyl)coumarin (**2**) was synthesized through a nucleophilic aromatic substitution reaction.

2.3.1. 7-Hydroxy-8-methyl-4-(2,3,4,5-tetrafluorophenyl)coumarin (**1**)

2-Methylresorcinol (1.17 g, 9.46 mmol) and ethyl-(2,3,4,5-tetrafluorobenzoyl)acetate (2.54 g, 9.46 mmol) were dissolved in a mixture of 5 mL CF₃COOH and 5 mL

H₂SO₄ at 0-5 °C for 24 hours. The reaction mixture was then cooled and precipitated with ice-cold water. The precipitate was filtered, washed with water until neutral, and allowed to dry. The crude product was finally purified by recrystallization from ethanol.

7-Hydroxy-8-methyl-4-(2,3,4,5-tetrafluorophenyl)coumarin (**1**) is soluble in chloroform, acetone, acetonitrile, ethyl acetate, *N,N*-dimethylformamide (DMF) and dimethyl sulfoxide (DMSO). Mp.: 173 °C. Yield: 2.71 g (88.37%). Anal. calculated for C₁₆H₈F₄O₃: C (59.28 %), H (2.48 %), F (23.44 %); found: C (59.26 %), H (2.48 %), F (23.46 %). UV-Vis, λ_{max} (1×10⁻⁵ M, in DMF) nm(log ε): 337 (4.32). FT-IR (ATR): ν_{max}/cm⁻¹: 3246 (Ar OH), 3066 (Ar C-H), 2913, 2921 (Aliphatic C-H), 1705 (Lactone C=O), 1481 (C=C). ¹H-NMR (400 MHz, DMSO-*d*₆) (δ: ppm) 10.63 (br s, 1H), 7.58-7.68 (m, 1H), 7.03 (dd, *J* = 8.5, 2 Hz, 1H), 6.84 (d, *J* = 8.7 Hz, 1H), 6.31 (s, 1H), 2.21 (s, 3H). ¹³C-NMR (400 MHz, DMSO-*d*₆) (δ: ppm) 8, 110, 111, 112, 113, 114, 120, 125, 139, 142, 143, 146, 148, 153, 160. ¹⁹F-NMR (400 MHz, DMSO-*d*₆) (δ: ppm) (-138.90)-(-139.04) (m, 2F), (-138.51)-(-138.65) (m, 2F).

2.3.2. 7-(2,3-Dicyanophenoxy)-8-methyl-4-(2,3,4,5-tetrafluorophenyl)coumarin (**2**)

7-Hydroxy-8-methyl-4-(2,3,4,5-tetrafluorophenyl)coumarin (**1**) (1.00 g, 3.08 mmol) and 3-nitrophthalonitrile (0.53 g, 3.08 mmol) were dissolved in 30 mL of anhydrous *N,N*-dimethylformamide. After stirring for 10 minutes, finely ground dry K₂CO₃ (0.64 g, 4.63 mmol) was added over 2 hours. The reaction mixture was then heated at 65 °C for 5 days under a nitrogen atmosphere. Once cooled to room temperature, the mixture was precipitated with ice-cold water. The resulting precipitate was filtered, washed with water until neutral, and allowed to dry. The crude product was purified by column chromatography using chloroform as the eluent and further purified by recrystallization from ethanol.

7-(2,3-Dicyanophenoxy)-8-methyl-4-(2,3,4,5-tetrafluorophenyl)coumarin (**2**) is soluble in methanol, ethanol, acetone, acetonitrile, chloroform, ethyl acetate, DMF, DMSO, and tetrahydrofuran (THF). Mp.: 240 °C. Yield: 0.91 g (65.46%). Anal. calculated for C₂₄H₁₀F₄N₂O₃: C (64.01 %), H (2.24 %), F (16.87 %), N (6.22 %); found: C (64.00 %), H (2.23 %), F (16.88 %), N (6.23 %). UV-Vis, λ_{max} (1×10⁻⁵ M, in DMF) nm(log ε): 319 (4.15). FT-IR (ATR): ν_{max}/cm⁻¹: 3073 (Ar C-H), 2975 (Aliphatic C-H), 2235 (C≡N), 1732 (Lactone C=O), 1590 (C=C), 1245 (Ar-O-Ar). ¹H-NMR (400 MHz, DMSO-*d*₆) (δ: ppm) 7.91 (d, *J* = 7.7 Hz, 1H), 7.86 (dd, *J* = 8.4 ve 8.5 Hz, 1H), 7.65-7.73 (m, 1H), 7.35 (d, *J* = 9.3 Hz, 1H), 7.32 (d, *J* = 8.7 Hz, 1H), 7.14 (br d, *J* = 8.5 Hz, 1H), 6.68 (s, 1H), 2.32 (s, 3H). ¹³C-NMR (400 MHz, DMSO-*d*₆) (δ: ppm) 10, 105, 113, 115, 115, 116, 116, 117, 117, 118, 119, 120, 122, 126, 129, 136, 146,

147, 153, 157, 155, 159, 160. ¹⁹F-NMR (400 MHz, DMSO-*d*₆) (δ: ppm) (-138.69)-(-138.84) (m, 2F), (-138.03)-(-138.17) (m, 2F).

2.3.3. 1(4),8(11),15(18),22(25)-Tetrakis-[7-oxy-8-methyl-4-(2,3,4,5-tetrafluorophenyl)coumarino] phthalocyaninato zinc (**II**) (**3**)

The phthalonitrile compound (**2**) (0.10 g, 0.05 mmol) and Zn(CH₃COO)₂·2H₂O (0.003 g, 0.013 mmol) were reacted in a reaction tube without solvent by heating with a heat gun up to 350 °C for 5 minutes. The reaction was monitored until a blue-green color appeared. At this point, 2 drops of anhydrous DMF were added, and the reaction was allowed to continue for an additional minute. Once the reaction was complete, 0.5 mL of anhydrous DMF was added to dissolve the solid formed. The resulting solution was then precipitated dropwise into ice-cold water. The precipitate was filtered through filter paper and allowed to dry. The precipitates were subsequently centrifuged and washed several times with hot water and methanol. Finally, the crude product was purified by column chromatography using chloroform (100:1) as the eluent.

1(4),8(11),15(18),22(25)-Tetrakis-[7-oxy-8-methyl-4-(2,3,4,5-tetrafluorophenyl)-coumarino] phthalocyaninato zinc (**II**) (**3**) is soluble in acetone, ethyl acetate, chloroform, acetonitrile, dichloromethane (DCM), DMF, DMSO and THF. Mp.: >300 °C. Yield: 0.008 g (32.00%). Anal. calculated for C₉₆H₄₀F₁₆N₈O₁₂Zn: C (61.77 %), H (2.16 %), F (16.28 %), N (6.00 %), Zn (3.50 %); found: C (61.76 %), H (2.15 %), F (16.29 %), N (6.02 %), Zn (3.49 %). UV-Vis, λ_{max} (1×10⁻⁵ M, in DMF) nm(log ε): 319 (5.21), 691 (5.16). FT-IR (ATR): ν_{max}/cm⁻¹: 3074 (Ar C-H), 2958, 2924, 2852 (Aliphatic C-H), 1726 (Lactone C=O), 1595 (C=C), 1264 (Ar-O-Ar). MALDI-TOF-MS *m/z*: Calc. 1866.75; found 1866.124 [M]⁺

2.3.4. 1(4),8(11),15(18),22(25)-Tetrakis-[7-oxy-8-methyl-4-(2,3,4,5-tetrafluorophenyl)coumarino] phthalocyaninato indium (**III**) acetate (**4**)

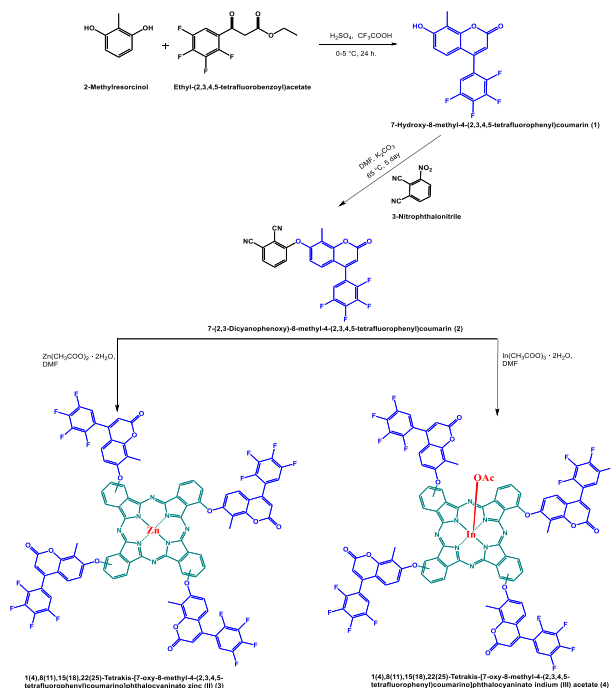
The phthalonitrile compound (**2**) (0.10 g, 0.05 mmol) and In(CH₃COO)₃·2H₂O (0.004 g, 0.013 mmol) were reacted by heating in a reaction tube without a solvent using a heat gun up to 370 °C for 10 minutes. The reaction continued until a blue-green color appeared, and then 2 drops of anhydrous DMF were added to the reaction mixture and allowed to continue for another minute. Once the reaction was complete, 0.5 mL of anhydrous DMF was added to dissolve the solid formed. The resulting substance was gradually added to ice-cold water to induce precipitation. The precipitate was then filtered through filter paper and allowed to dry. Next, the precipitate was centrifuged and washed multiple times with hot water and methanol. Finally, the crude product

was purified by column chromatography with chloroform (100:1) as the eluent.

1(4),8(11),15(18),22(25)-Tetrakis-[7-oxy-8-methyl-4-(2,3,4,5-tetrafluorophenyl)-coumarino]phthalocyaninato indium (II) acetate (**4**) is soluble in acetone, chloroform, acetonitrile, ethyl acetate, DCM, DMF, DMSO and THF. Mp.: >300 °C. Yield: 0.0010 g (37.04%). Anal. calculated for $C_{96}H_{43}F_{16}InN_8O_{14}$: C (59.59 %), H (2.19 %), F (15.39 %), In (5.81 %), N (5.67 %); found: C (59.58 %), H (2.17 %), F (15.40 %), In (5.82 %), N (5.68 %). UV-Vis, λ_{max} (1×10^{-5} M, in DMF) nm(log ϵ): 319 (4.92), 704 (4.73). FT-IR (ATR): ν_{max}/cm^{-1} : 3071 (Ar C–H), 2927, 2857 (Aliphatic C–H), 1724 (Lactone C=O), 1596 (C=C), 1262 (Ar–O–Ar). MALDI-TOF-MS m/z: Calc. 1975.23; found 2106,132 $[M+CHCA+H-OAc]^+$

3. Results and Discussion

The synthesis schemes for non-peripheral zinc and indium phthalocyanines containing 7-hydroxy-8-methyl-4-(2,3,4,5-tetrafluorophenyl)coumarin are illustrated in **Scheme 1**.



Scheme 1. Synthesis of coumarin (**1**), its phthalonitrile derivative (**2**), and phthalocyanine derivatives (**3**, **4**).

7-Hydroxy-8-methyl-4-(2,3,4,5-tetrafluorophenyl)coumarin (**1**) was synthesized via the Pechmann reaction using 2-methylresorcinol and ethyl-(2,3,4,5-tetrafluorobenzoyl)acetate in the presence of H_2SO_4 and CF_3COOH at 0-5 °C. The phthalonitrile derivative of this coumarin (**1**) was synthesized through a nucleophilic aromatic substitution reaction in anhydrous N,N -dimethylformamide using 3-nitrophthalonitrile.

Non-peripheral zinc(II) and indium (III) acetate phthalocyanine (**3,4**) derivatives were prepared through cyclotetramerization of the coumarin-phthalonitrile derivative compound. Coumarin-substituted zinc(II) and indium (III) phthalocyanines were prepared by heating in the absence of solvent at temperatures exceeding 350 °C in the presence of zinc (II) acetate and indium (III) acetate. Column chromatography was used to purify each and every product that was produced.

Phthalocyanine complexes without substituents typically have poor solubility in organic solvents. However, literature indicates that phthalocyanines containing polar groups generally exhibit good solubility. It was observed that the synthesized zinc and indium metallophthalocyanines showed good solubility in organic solvents such as ethyl acetate, acetonitrile, chloroform, DCM, DMF, THF, and DMSO.

The newly synthesized compounds were characterized using elemental analysis, FT-IR, UV-Vis, 1H -NMR, ^{13}C -NMR, ^{19}F -NMR, and MALDI-TOF-MS spectroscopic techniques. In the FT-IR spectra of the compounds, the characteristic carbonyl ($-C=O$) peak of the coumarin compound (**1**) was observed around 1705 cm^{-1} , while the hydroxyl ($-OH$) peak appeared at approximately 3246 cm^{-1} . The hydroxyl ($-OH$) peak was absent in the FT-IR spectrum of the coumarin phthalonitrile derivative (**2**). The $-C\equiv N$ peak for the coumarin phthalonitrile derivative (**2**) was detected at 2235 cm^{-1} , and the Ar–O–Ar peak was seen around 1245 cm^{-1} . The disappearance of the hydroxyl ($-OH$) peak and the appearance of the $-C\equiv N$ and Ar–O–Ar peaks indicate the successful formation of the phthalonitrile derivative. After conversion to phthalocyanines, the $-C\equiv N$ peak, typically observed at 2235 cm^{-1} in phthalonitrile derivatives, was no longer present. The absence of $-C\equiv N$ peaks in all phthalocyanine derivatives confirms the formation of the phthalocyanine compounds.

MALDI-TOF mass spectrometry is a crucial technique for determining the molecular weights of phthalocyanine complexes. In the mass spectra of all phthalocyanines, the molecular weights were observed as $[M]^+$ or $[M+CHCA+H-OAc]^+$. Positive ion and linear mode MALDI-TOF mass spectra were acquired using 2,5-dihydroxybenzoic acid (DHB) or dithranol (DIT) as the MALDI matrix. The proposed structures of the phthalocyanine compounds align with the results obtained from elemental analysis.

3.1. Spectrophotometric and Fluorometric Properties of Phthalocyanines

Phthalocyanines display Q and B band absorptions in the UV-visible region, making them amenable to characterization by UV-Vis spectroscopy. The basic electronic absorption spectra of non-peripheral tetra zinc and indium phthalocyanine compounds typically feature a narrow Q band in the range of 650-705 nm. The

presence of Zn and In metals in the phthalocyanine cores does not cause significant broadening of the Q band. Phthalocyanine compounds substituted with non-peripheral coumarin derivatives, along with zinc and indium metals, exhibit good solubility in solvents such as acetone, ethyl acetate, DCM, DMF, DMSO, and THF. When assessing the solvent effects on phthalocyanines, the most pronounced bathochromic shift was observed in DMSO compared to DCM, while the most significant hypsochromic shift was noted in ethyl acetate and acetone (Figure 1).

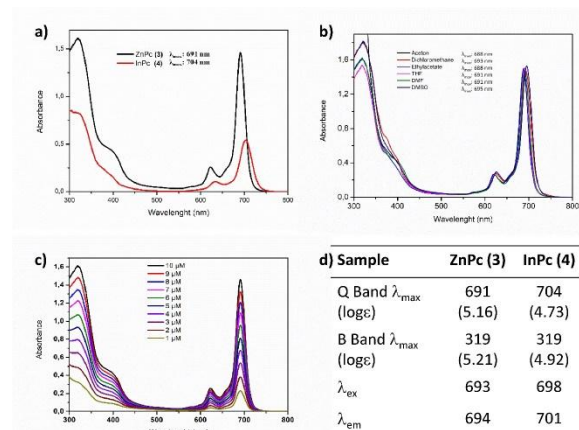


Figure 1. a) UV-Vis comparison of synthesized phthalocyanines in DMF. b) UV-Vis comparison of compound (3) in different solvents. c) UV-Vis spectra of compound (3) at ten different concentrations in DMF. d) UV-Vis and fluorescence data of phthalocyanine compounds (3) and (4).

The aggregation behavior of the phthalocyanine compounds at various concentrations in DMF was investigated due to the significant absorption of the produced compounds in DMF. In non-peripheral coumarin-substituted zinc and indium phthalocyanines, it was found that the intensity of the Q band increased with increasing concentration and that no aggregation was seen. The Lambert-Beer law was found to be satisfied by all phthalocyanine compounds within the concentration range of 1×10^{-5} to 1×10^{-6} M (in DMF) (Figure 1).

3.2. Singlet Oxygen Quantum Yields

Singlet oxygen quantum yields (Φ_{Δ}) for zinc (II) and indium (III) acetate phthalocyanines, substituted with fluoro-phenyl coumarin, were assessed using a spectrophotometric approach with 1,3-diphenylisobenzofuran (DPBF) as a quencher. The analysis revealed changes in the Q band during the measurement of singlet oxygen quantum yields. To avoid the quenching effect of DMSO, singlet oxygen measurements were performed in DMF. It was observed that zinc (II) phthalocyanine derivatives, featuring non-peripheral coumarin at the fluorophenyl position, exhibited enhanced stability to light compared to their indium (III) acetate counterparts, showing less

degradation with extended exposure. This is attributed to zinc (II) metal being smaller in size compared to indium (III) acetate metal, allowing it to fit snugly into the center of the phthalocyanine skeleton and form stable coordination bonds. Conversely, the indium (III) acetate phthalocyanine compound, due to the indium (III) acetate metal not fitting perfectly into the center and the electron-withdrawing properties of the acetate group, reduces the reactivity at the core of the phthalocyanine, rendering the phthalocyanine compound less stable against singlet oxygen [42], [43] (Table 1).

Table 1. Photophysical and photochemical parameters of phthalocyanines (3,4) in DMF.

	λ_{max}	log ϵ	Φ_{Δ}	Φ_d
3	691	(5.16)	0.55	1.09
4	704	(4.73)	0.80	7.32
ZnPc⁽⁴⁴⁾	670	(5.37)	0.56	0.023
InPc⁽⁴⁴⁾	683	(4.93)	0.75	0.54

In our study of synthesized coumarin-substituted phthalocyanine derivatives, we observed that the indium metal phthalocyanine derivative (4) in the non-peripheral position exhibits a higher singlet oxygen quantum yield ($\Phi_{\Delta} = 0.803$) compared to the zinc metal phthalocyanine derivative (3) ($\Phi_{\Delta} = 0.547$). This increase in Φ_{Δ} for the indium derivative can be attributed to several factors. Firstly, in non-peripheral substituted phthalocyanine derivatives, the substituents are positioned closer to the phthalocyanine center, facilitating easier electron transfer. Secondly, indium, being a heavier atom compared to zinc, induces a heavier atom effect which enhances the production of singlet oxygen. This is because the heavier atom effect in indium increases spin-orbit coupling, promoting intersystem crossing to the triplet state.

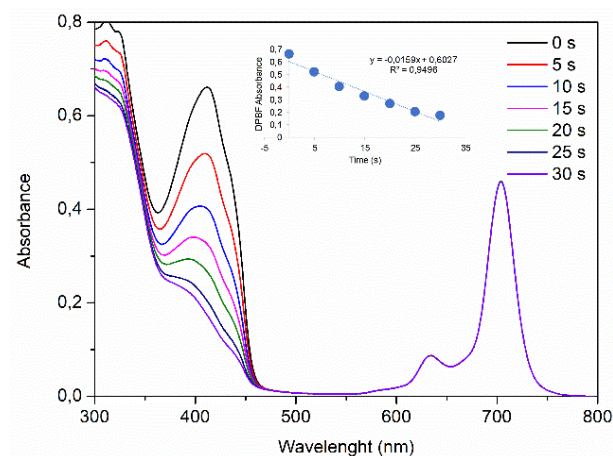


Figure 2. Time-dependent decrease in absorption of the DPBF compound in DMF, over 5 seconds, with compound (4) used to determine the singlet oxygen quantum yield (concentration $\sim 10 \mu\text{M}$).

Consequently, this mechanism enhances the production of singlet oxygen, as excited electrons in heavy metal atoms such as indium have an increased propensity for intersystem transitions rather than losing energy through emission. For comparison, the singlet oxygen quantum yields of all the synthesized complexes were measured relative to the standard zinc phthalocyanine (ZnPc) compound, which has a Φ_{Δ} of 0.56 in DMF [44]. The results clearly demonstrate the superior efficiency of the indium-substituted phthalocyanine derivative in generating singlet oxygen [45], [46] (Figure 2).

3.3. Photodegradation Quantum Yields

The decay of a substance caused by light radiation is known as photodegradation. One crucial aspect of photochemistry is a compound's resistance to light. When assessing the light sensitivity of photosensitizers used in the pharmaceutical industry, the photodegradation quantum yield (Φ_d) is an essential measure. This yield should ideally be in the range of 10^{-3} to 10^{-6} M [47]. The coumarin-phthalocyanine photosensitizer assaults the phthalocyanine ring and disintegrates its skeleton when exposed to strong light by producing singlet oxygen. The Q band gets smaller as a result of this process. Degrading the photosensitizer is crucial in order to help the body remove it for use in photodynamic treatment. Every photodegradation investigation was carried out in DMF (Figure 3).

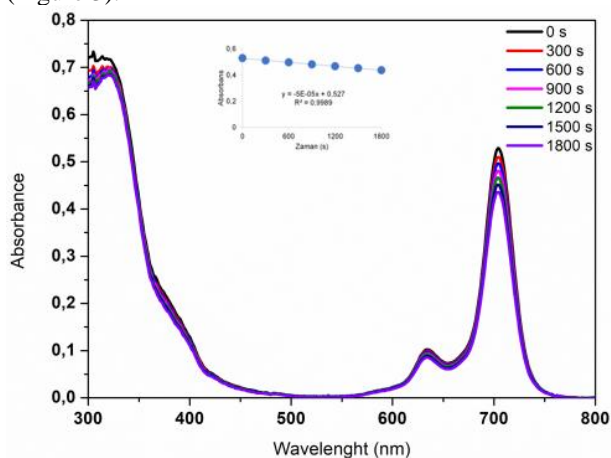


Figure 3. The absorption photodegradation spectrum of compound (4) under light irradiation for 1800 seconds. (Concentration $\sim 10 \mu\text{M}$).

The zinc (II) phthalocyanine compound substituted with coumarin at non-peripheral positions is more stable to light and exhibits less degradation under prolonged exposure compared to its indium (III) acetate phthalocyanine derivative. This is because zinc (II) metal is smaller in size than indium (III) acetate metal and forms stable coordination bonds by fitting precisely into the core of the phthalocyanine skeleton. However, the indium (III) acetate phthalocyanine compound reduces reactivity in the core of the phthalocyanine due to the indium (III) acetate metal not fitting into the core and the electron-withdrawing properties of the acetate group,

making the phthalocyanine compound less stable against singlet oxygen.

4. Conclusion

In conclusion, non-peripheral zinc (II) and indium (III) acetate phthalocyanine complexes were successfully synthesized from 7-hydroxy-8-methyl-4-(2,3,4,5-tetrafluorophenyl)coumarin. These novel compounds were characterized by using a range of techniques, including elemental analysis, UV-visible, FT-IR spectroscopy, and MALDI-TOF mass spectrometry. The aggregation behavior, singlet oxygen quantum yields, and photodegradation quantum yields of these new phthalocyanines were investigated in DMF. The compounds demonstrated excellent solubility in common organic solvents and exhibited photophysical and photochemical properties comparable to previously studied phthalocyanine derivatives. Notably, the indium (III) acetate phthalocyanine derivative showed a higher singlet oxygen quantum yield than the zinc (II) derivative. These results suggest that coumarin-phthalocyanine complexes have potential as photosensitizers in photodynamic therapy and may benefit from further development through targeted modifications.

Acknowledgement

We gratefully acknowledge the Research Foundation of Marmara University, Commission of Scientific Research Project (BAPKO) for their support under grant FYL-2022-10633.

Author's Contributions

Zehra Kazancıçok: Drafted and wrote the manuscript, performed the experiment and result analysis.

Mustafa Bulut: Drafted and wrote the manuscript.

Ümit Salan: Assisted in analytical analysis on the structure, supervised the experiment's progress, result interpretation and helped in manuscript preparation.

Ethics

There are no ethical issues after the publication of this manuscript.

References

- [1]. Yahya, M., Nural, Y., & Seferoğlu, Z. (2022). Recent advances in the nonlinear optical (NLO) properties of phthalocyanines: A review. *Dyes and Pigments*, 198, 109960. (<https://doi.org/10.1016/j.dyepig.2021.109960>)
- [2]. Claessens, C. G., Hahn, U. W. E., & Torres, T. (2008). Phthalocyanines: From outstanding electronic properties to emerging applications. *The Chemical Record*, 8(2), 75-97. (<https://doi.org/10.1002/tcr.20139>)

- [3]. Klyamer, D., Bonegardt, D., & Basova, T. (2021). Fluoro-substituted metal phthalocyanines for active layers of chemical sensors. *Chemosensors*, 9(6), 133. (<https://doi.org/10.3390/chemosensors9060133>)
- [4]. Song, C., Li, Y., Gao, C., Zhang, H., Chuai, Y., & Song, D. (2020). An OTFT based on titanium phthalocyanine dichloride: A new p-type organic semiconductor. *Materials Letters*, 270, 127666. (<https://doi.org/10.1016/j.matlet.2020.127666>)
- [5]. Molina, D., Follana-Berná, J., & Sastre-Santos, Á. (2023). Phthalocyanines, porphyrins and other porphyrinoids as components of perovskite solar cells. *Journal of Materials Chemistry C*, 11(24), 7885-7919. (<https://doi.org/10.1039/D2TC04441B>)
- [6]. Rezaee, E., Khan, D., Cai, S., Dong, L., Xiao, H., Silva, S. R. P., Liu, X., & Xu, Z. X. (2023). Phthalocyanine in perovskite solar cells: A review. *Materials Chemistry Frontiers*, 7(9), 1704-1736. (<https://doi.org/10.1039/D2QM01369J>)
- [7]. Yabaş, E., Biçer, E., & Altındal, A. (2023). Novel reduced graphene oxide/zinc phthalocyanine and reduced graphene oxide/cobalt phthalocyanine hybrids as high sensitivity room temperature volatile organic compound gas sensors. *Journal of Molecular Structure*, 1271, 134076. (<https://doi.org/10.1016/j.molstruc.2022.134076>)
- [8]. Gursel, Y. H., Senkal, B. F., Kandaz, M., & Yakuphanoglu, F. (2009). Synthesis and liquid crystal properties of phthalocyanine bearing a star polytetrahydrofuran moiety. *Polyhedron*, 28(8), 1490-1496. (<https://doi.org/10.1016/j.poly.2009.02.038>)
- [9]. Canımurbey, B., Taşkan, M. C., Demir, S., Duygulu, E., Atilla, D., & Yuksel, F. (2020). Synthesis and investigation of the electrical properties of novel liquid-crystal phthalocyanines bearing triple branched alkylthia chains. *New Journal of Chemistry*, 44(18), 7424-7435. (<https://doi.org/10.1039/D0NJ00678E>)
- [10]. Balamurugan, G., & Park, J. S. (2022). Enhanced solution processing and optical properties of perhalogenated zinc-phthalocyanines via anion- π bonding. *Dyes and Pigments*, 201, 110199. (<https://doi.org/10.1016/j.dyepig.2022.110199>)
- [11]. Lo, P. C., Rodríguez-Morgade, M. S., Pandey, R. K., Ng, D. K., Torres, T., & Dumoulin, F. (2020). The unique features and promises of phthalocyanines as advanced photosensitizers for photodynamic therapy of cancer. *Chemical Society Reviews*, 49(4), 1041-1056. (<https://doi.org/10.1039/C9CS00129H>)
- [12]. Zhang, Y., & Lovell, J. F. (2017). Recent applications of phthalocyanines and naphthalocyanines for imaging and therapy. *Wiley Interdisciplinary Reviews: Nanomedicine and Nanobiotechnology*, 9(1), e1420. (<https://doi.org/10.1002/wnan.1420>)
- [13]. Çalık, A. E., Köksoy, B., Orman, E. B., Durmuş, M., Özkaya, A. R., & Bulut, M. (2013). 4-Carboxymethyl-8-methyl-7-oxycoumarin substituted zinc, cobalt and indium phthalocyanines: Electrochemical and photochemical properties. *Journal of Porphyrins and Phthalocyanines*, 17(10), 1046-1054. (<https://doi.org/10.1142/S108842461350096X>)
- [14]. Saka, E. T., Göl, C., Durmuş, M., Kantekin, H., & Bıyıklıoğlu, Z. (2012). Photophysical, photochemical and aggregation behavior of novel peripherally tetra-substituted phthalocyanine derivatives. *Journal of Photochemistry and Photobiology A: Chemistry*, 241, 67-78. (<https://doi.org/10.1016/j.jphotochem.2012.05.023>)
- [15]. Prabhu CP, K., Nemakal, M., Managa, M., Nyokong, T., & Koodlur Sannegowda, L. (2021). Symmetrically substituted Zn and Al phthalocyanines and polymers for photodynamic therapy application. *Frontiers in Chemistry*, 9, 647331. (<https://doi.org/10.3389/fchem.2021.647331>)
- [16]. Neagu, M., Constantin, C., Tampa, M., Matei, C., Lupu, A., Manole, E., Ion, R.M., Fenga, C., & Tsatsakis, A. M. (2016). Toxicological and efficacy assessment of post-transition metal (Indium) phthalocyanine for photodynamic therapy in neuroblastoma. *Oncotarget*, 7(43), 69718. (<https://doi.org/10.18632/oncotarget.11942>)
- [17]. Özdemir, M., Köksoy, B., Yalçın, B., Taşkın, T., Selçuki, N. A., Salan, Ü., Durmuş, M., & Bulut, M. (2021). Novel lutetium (III) phthalocyanine-coumarin dyads; synthesis, characterization, photochemical, theoretical and antioxidant properties. *Inorganica Chimica Acta*, 517, 120145. (<https://doi.org/10.1016/j.ica.2020.120145>)
- [18]. Sharma, D., Steen, G., Korterik, J. P., García-Iglesias, M., Vázquez, P., Torres, T., Herek, J. L., & Huijser, A. (2013). Impact of the anchoring ligand on electron injection and recombination dynamics at the interface of novel asymmetric push-pull zinc phthalocyanines and TiO₂. *The Journal of Physical Chemistry C*, 117(48), 25397-25404. (<https://doi.org/10.1021/jp410080a>)
- [19]. Kwiatkowski, S., Knap, B., Przystupski, D., Saczko, J., Kędzierska, E., Knap-Czop, K., Kotlińska, J., Michel, O., Kotowski, K., & Kulbacka, J. (2018). Photodynamic therapy-mechanisms, photosensitizers and combinations. *Biomedicine & pharmacotherapy*, 106, 1098-1107. (<https://doi.org/10.1016/j.biopha.2018.07.049>)
- [20]. Köksoy, B., Durmuş, M., & Bulut, M. (2019). Potential photosensitizer candidates for PDT including 7-oxy-3-thiomethylphenyl coumarino-phthalocyanines. *Inorganica Chimica Acta*, 498, 119137. (<https://doi.org/10.1016/j.ica.2019.119137>)
- [21]. Rak, J., Kabesova, M., Benes, J., Pouckova, P., & Vetvicka, D. (2023). Advances in liposome-encapsulated phthalocyanines for photodynamic therapy. *Life*, 13(2), 305. (<https://doi.org/10.3390/life13020305>)
- [22]. Supuran, C. T. (2020). Coumarin carbonic anhydrase inhibitors from natural sources. *Journal of Enzyme Inhibition and Medicinal Chemistry*, 35(1), 1462-1470. (<https://doi.org/10.1080/14756366.2020.1788009>)
- [23]. Özdemir, M., Taşkın, D., Ceyhan, D., Köksoy, B., Taşkın, T., Bulut, M., & Yalçın, B. (2023). 7, 8-Dihydroxycoumarin derivatives: In silico molecular docking and in vitro anticholinesterase activity. *Journal of Molecular Structure*, 1274, 134535. (<https://doi.org/10.1016/j.molstruc.2022.134535>)
- [24]. Mishra, S., Pandey, A., & Manvati, S. (2020). Coumarin: An emerging antiviral agent. *Heliyon*, 6(1). (<https://doi.org/10.1016/j.heliyon.2020.e03217>)
- [25]. Qin, H. L., Zhang, Z. W., Ravindar, L., & Rakesh, K. P. (2020). Antibacterial activities with the structure-activity relationship of coumarin derivatives. *European journal of medicinal chemistry*, 207, 112832. (<https://doi.org/10.1016/j.ejmech.2020.112832>)
- [26]. Ramsis, T. M., Ebrahim, M. A., & Fayed, E. A. (2023). Synthetic coumarin derivatives with anticoagulation and antiplatelet aggregation inhibitory effects. *Medicinal Chemistry Research*, 32(11), 2269-2278. (<https://doi.org/10.1007/s00044-023-03148-1>)
- [27]. Todorov, L., Saso, L., & Kostova, I. (2023). Antioxidant activity of coumarins and their metal complexes. *Pharmaceuticals*, 16(5), 651. (<https://doi.org/10.3390/ph16050651>)
- [28]. Çelik, E., Özdemir, M., Köksoy, B., Taskin-Tok, T., Taslimi, P., Sadeghian, N., & Yalçın, B. (2023). New Coumarin-Thiosemicarbazone Based Zn (II), Ni (II) and Co (II) Metal Complexes: Investigation of Cholinesterase, α -Amylase, and α -Glucosidase Enzyme Activities, and Molecular Docking Studies. *ChemistrySelect*, 8(38), e202301786. (<https://doi.org/10.1002/slct.202301786>)
- [29]. Rawat, A., & Reddy, A. V. B. (2022). Recent advances on anticancer activity of coumarin derivatives. *European Journal of Medicinal Chemistry Reports*, 5, 100038. (<https://doi.org/10.1016/j.ejmcr.2022.100038>)

- [30]. Bisi, A., Cappadone, C., Rampa, A., Farruggia, G., Sargenti, A., Belluti, F., Di Martino, R. M. C., Malucelli, E., Meluzzi, A., Iotti, S., & Gobbi, S. (2017). Coumarin derivatives as potential antitumor agents: Growth inhibition, apoptosis induction and multidrug resistance reverting activity. *European journal of medicinal chemistry*, 127, 577-585. (<https://doi.org/10.1016/j.ejmech.2017.01.020>)
- [31]. Çamur, M., Durmuş, M., & Bulut, M. (2012). Highly singlet oxygen generative water-soluble coumarin substituted zinc (II) phthalocyanine photosensitizers for photodynamic therapy. *Polyhedron*, 41(1), 92-103. (<https://doi.org/10.1016/j.poly.2012.04.034>)
- [32]. Dandriyal, J., Singla, R., Kumar, M., & Jaitak, V. (2016). Recent developments of C-4 substituted coumarin derivatives as anticancer agents. *European journal of medicinal chemistry*, 119, 141-168. (<https://doi.org/10.1016/j.ejmech.2016.03.087>)
- [33]. Roh, E. J. (2021). Inhibitory effects of coumarin derivatives on tyrosinase. *Molecules*, 26(8), 2346. (<https://doi.org/10.3390/molecules26082346>)
- [34]. Deng, G., Xu, H., Kuang, L., He, C., Li, B., Yang, M., Zhang, X., Li, Z., & Liu, J. (2019). Novel nonlinear optical chromophores based on coumarin: Synthesis and properties studies. *Optical Materials*, 88, 218-222. (<https://doi.org/10.1016/j.optmat.2018.11.035>)
- [35]. Liu, X., Cole, J. M., Waddell, P. G., Lin, T. C., Radia, J., & Zeidler, A. (2012). Molecular origins of optoelectronic properties in coumarin dyes: toward designer solar cell and laser applications. *The Journal of Physical Chemistry A*, 116(1), 727-737. (<https://doi.org/10.1021/jp209925y>)
- [36]. Pradhan, R., Khandelwal, K., Shankar S, S., Panda, S. J., Purohit, C. S., Bag, B. P., Singhal, R., Liu, W., Zhu, X., Sharma, G. D., & Mishra, A. (2023). Correlation of Functional Coumarin Dye Structure with Molecular Packing and Organic Solar Cells Performance. *Solar RRL*, 7(21), 2300487. (<https://doi.org/10.1002/solr.202300487>)
- [37]. Köksoy, B., Durmuş, M., & Bulut, M. (2015). Tetra-and octa-[4-(2-hydroxyethyl) phenoxy bearing novel metal-free and zinc (II) phthalocyanines: Synthesis, characterization and investigation of photophysical and photochemical properties. *Journal of Luminescence*, 161, 95-102. (<https://doi.org/10.1016/j.jlumin.2014.12.044>)
- [38]. Zhou, X. Q., Meng, L. B., Huang, Q., Li, J., Zheng, K., Zhang, F. L., Liu, J. Y., & Xue, J. P. (2015). Synthesis and in vitro anticancer activity of zinc (II) phthalocyanines conjugated with coumarin derivatives for dual photodynamic and chemotherapy. *ChemMedChem*, 10(2), 304-311. (<https://doi.org/10.1002/cmde.201402401>)
- [39]. Boyar, C. Y., & Çamur, M. (2019). Novel water soluble 7-oxy-4-(pyridine-3-yl) coumarin substituted phthalocyanines as potential photosensitizers for photodynamic therapy. *Inorganica Chimica Acta*, 494, 30-41. (<https://doi.org/10.1016/j.ica.2019.05.004>)
- [40]. J.G. Young, W. Onyebuagu, Synthesis and characterization of di-disubstituted phthalocyanines, *The Journal of Organic Chemistry* 55(7) (1990) 2155-2159. (<https://doi.org/10.1021/jo00294a032>)
- [41]. George, R. D., & Snow, A. W. (1995). Synthesis of 3-nitrothalonitrile and tetra- α -substituted phthalocyanines. *Journal of Heterocyclic Chemistry*, 32(2), 495-498. (<https://doi.org/10.1002/jhet.5570320219>)
- [42]. Dyrda, G. (2023). Photostability of indium phthalocyanines in organic solvents. (<https://doi.org/10.21203/rs.3.rs-3407051/v1>)
- [43]. Gürel, E., Pişkin, M., Altun, S., Odabaş, Z., & Durmuş, M. (2015). Synthesis, characterization and investigation of the photophysical and photochemical properties of highly soluble novel metal-free, zinc (II), and indium (III) phthalocyanines substituted with 2, 3, 6-trimethylphenoxy moieties. *Dalton Transactions*, 44(13), 6202-6211. (<https://doi.org/10.1039/C5DT00304K>)
- [44]. Özdemir, M., Karapınar, B., Yalçın, B., Salan, Ü., Durmuş, M., & Bulut, M. (2019). Synthesis and characterization of novel 7-oxy-3-ethyl-6-hexyl-4-methylcoumarin substituted metallo phthalocyanines and investigation of their photophysical and photochemical properties. *Dalton Transactions*, 48(34), 13046-13056. (<https://doi.org/10.1039/C9DT02687H>)
- [45]. Güzel, E., Arslan, B. S., Atmaca, G. Y., Nebioğlu, M., & Erdoğan, A. (2019). High photosensitized singlet oxygen generating zinc and chloroindium phthalocyanines bearing (4-isopropylbenzyl) oxy groups as potential agents for photophysical and photochemical applications. *ChemistrySelect*, 4(2), 515-520. (<https://doi.org/10.1016/j.jphotochem.2015.10.026>)
- [46]. Yaşa Atmaca, G., & Erdoğan, A. (2017). Novel, Highly Soluble Non-Peripherally Phthalocyanines Bearing Bulky Groups Containing Fluorine Atoms: Synthesis, Characterization, Spectral and Improved Photophysical and Photochemical Properties. *Hacettepe Journal of Biology and Chemistry*, 45(1). (10.15671/HJBC.2017.137)
- [47]. Karapınar, B., Özdemir, M., Salan, Ü., Durmuş, M., Yalçın, B., & Bulut, M. (2019). 7-Oxy-3, 4-cyclohexenecoumarin Carrying Novel Zinc (II) and Indium (III) Acetate Phthalocyanines: Synthesis, Characterization, Photophysical and Photochemical Properties. *Chemistry Select*, 4(33), 9632-9639. (<https://doi.org/10.1002/slct.201902582>)